Al-Rafidain Journal of Engineering Sciences

Journal homepage https://rjes.iq/index.php/rjes

ISSN 3005-3153 (Online)

Exergoeconomic and Exergoenvironmental Analysis of a Solar–Geothermal Integrated Multigeneration System for Power, Cooling, and Hydrogen Production

Falah Hassan Mohammed

Assistant Governor for planning Affairs, Wasit, Iraq

ARTICLE INFO

Article history:

Received 19 December 2025
Revised 19 December 2025,
Accepted 04 January 2026,
Available online 18 January 2026

Keywords:

Solar–geothermal integration
Multigeneration system
Exergy analysis
Exergoeconomic analysis
Exergoenvironmental analysis

ABSTRACT

The exergy, exergoeconomic, and exergoenvironmental analyses of a solar–geothermal integrated multigeneration system with electricity synthesis (e.g., electric, cooling, and hydrogen) are described here. It comprises a solar thermal collector, geothermal heat exchanger, turbine–generator, condenser, absorption chiller, and electrolyzer. The exergy analyzes total exergy destruction of the system, 625 kW, with the condenser contributing more irreversibility (550 kW, 88% of the total), geothermal heat exchanger (300 kW) and turbine–generator (80 kW). On the other hand, the solar collector and absorption chiller show negative exergy destruction values (−300 kW and −70 kW). Electrolyzer $\eta_{ex} \approx 24$ (highest exergetic efficiency), condenser $\eta_{ex} \approx 0.19$ (lowest efficiency). From the exergoeconomic analysis, hydrogen is the economy with the highest unit exergy cost (≈166.7 \$/GJ_{ex}) with a cost rate of 0.02 \$/s, and this can be concluded as an economically intensive product. Geothermal heat exchanger has high exergoeconomic component $f \approx 0.97$ which means that the performance is more dependent on investment capital than thermodynamic cost. The turbine–generator and geothermal heat exchanger exhibit the highest environmental impact rates (≈0.0012 and 0.0006 pts/s, respectively) from a structural perspective while the hydrogen product has the highest unit environmental impact (≈8.33 pts/GJ_{ex}). In conclusion, all identified results show that condenser irreversibility, electrolyzer cost and geothermal heat exchanger impacts are the most important sustainability problems faced. The results offer quantitative suggestions for system optimization considering the thermodynamic efficiency, economic feasibility and environmental performance of the solar–geothermal multigeneration systems as systems to be improved.

1. Introduction

More than ever, with growing energy consumption worldwide as well as climate change, resource depletion, environmental degradation and other issues, the desire for efficient and sustainable energy systems becomes critical. Traditional single-generation energy plants suffer from low overall efficiency as a significant portion of the supplied energy is rejected as waste heat. This has made multigeneration schemes where electricity, heating or cooling, and hydrogen production are generated simultaneously an efficient solution to increase energy efficiency and cut environmental losses. Solar and geothermal energies are also particularly well understood as renewable resources with great potential for renewable energy, as they are abundant, emit little, and complement each other. Solar delivers high-quality thermal energy but is intermittent by nature and geothermal energy provides a constant temperature renewable heat source with low

Corresponding author E-mail address: falah.hassanm1976@gmail.com
https://doi.org/10.61268/t10aeq16

fluctuation in usage and provides reliable thermal energy. Combining these two resources in a single entity can greatly enhance reliability and flexibility of operation while providing better penetration of renewable energy sources. Solar–geothermal hybrid multigeneration systems are therefore a bright prospect in the development of sustainable energy systems. Exergy analysis using a classical energy model based on the first law of thermodynamics can offer an understanding of an energy quantity, yet it does not take into consideration the quality of the energy and irreversibilities of energy in the system. An energy analysis inspired by the second law of thermodynamics will overcome this limitation, by specifying the origins of an irreversibility and its magnitude, and determining the performance of the system part (i.e., thermodynamic efficiency alone, however, is not enough to inform real-world system design. With this background, exergoeconomic analysis is created to link the destruction of exergy with its economic implications so that can select economically intensive components and economically optimal strategies to facilitate improvement. Exergoenvironmental analysis, moreover, broadens the exergy framework by connecting environmental impacts to exergy flows, thus offering a strong instrument for assessing sustainability and environmental efficiency.

(Abdulsitar et al., 2025) [1] conducted a thorough energy, exergy, exergoeconomic, and exergoenvironmental assessment of a combined cycle power plant. Their findings reveal the major drivers of irreversibilities, and show that integrated exergetic and economic analyses can provide fruitful paths toward plant sustainability and cost efficiency. (Agberegha & Nwigbo, 2024) [2] devised an integrated energy, exergy, exergoeconomic, and exergoenvironmental model of a multigeneration power plant. Their results indicated that integration of the systems greatly improves overall efficiencies and reduces environmental and operating costs. (Assareh et al., 2022) [3] developed a geothermal- and solar-based multigeneration system for the generation of clean power and hydrogen. The research underscored the superior performance of hybrid renewable sources in alleviating the energy–water–hydrogen nexus for improved thermodynamic performance. (Azizi et al., 2022) [4] offered a critical overview of energy, exergy and economics of multigeneration systems based on geothermal electricity. Their review highlighted that the reliability and sustainability of geothermal resources is very satisfactory, and their combination with advanced optimization techniques was mentioned as a strength, especially for advanced optimization methods. (Bahrami & Rosen, 2024) [5] carried out an exergoeconomic assessment and multidimensional optimization of a new low-temperature geothermal system that would provide cooling, electricity, and hydrogen. They verified that zero-emission systems could be developed in light of low-grade geothermal resources. (Chen et al., 2021) [6] studied the energy, exergy, and exergoenvironmental characteristics for the coupling of electrochemical copper–chlorine cycle with Goswami cycle. System coupling enhances the efficiency of the hydrogen production with less environmental load, as shown by this work. (Chen et al., 2025) [7] studied a photovoltaic–hydrogen co-generation PV–polygeneration system for green data centers. Their energy, economic, and environmental evaluations demonstrated substantial decreases in carbon dioxide emissions and operating expenses compared to traditional power supply systems. (Cui & Aziz, 2024) [8] carried out thermodynamic and economic analyses for geothermal-based hydrogen energy systems. Their results showed that geothermal could represent an economical and environmentally friendly alternative to the large-scale hydrogen production of large-scale hydrogen energy systems and low cost and green. (Demir et al., 2024) [9] identified a low-carbon multigeneration plan that integrates solar collectors, bio-waste gasification and water capture units. The research also recorded significant gains in general efficiency and reductions in greenhouse gas emissions. (Frank & Effiom, 2023) [10] established a multigeneration hydrogen production-integrated system to study its thermodynamics.

In their analysis, they provided evidence that the existing system can drive both the energy utilization and the clean fuel generation into the future. (Habibzadeh et al., 2023) [11] designed solar and geothermal-induced multigeneration system augmented by TiO_2 and SiO_2 nanoparticles. Results: The performances on heat transfer enhancement and energy saving in general could be attributed to the nanofluids. (Haider et al., 2023) [12] demonstrated a geothermal-enhanced multigeneration system developed for a sustainable urban setup. The system's energy and exergy results confirmed the potential role of system to support sustainable urban infrastructure with lower emissions. (Jalili et al., 2021) [13] conducted exergetic, exergoeconomic, and exergoenvironmental analysis of a trigeneration system powered by biomass and natural gas. Higher efficiency and less environmental consequences are the benefits of hybrid fuel usage, the study emphasized. (Li et al., 2024) [14] studied green hydrogen production increase using an integrated double-flash geothermal cycle. For advanced geothermal system design, they achieved an improved hydrogen yield and lower environmental impact by multi-criteria optimization. (Lotfalipour et al., 2025) [15] put forward an integrative framework to combine economic and environmental analyses to power generation and desalination via solar and geothermal resources. Their study highlighted strong synergies between renewable energy integration and sustainable water–energy systems. (Luo & Taghavi, 2024) [16] studied the environmental and exergoeconomic performance of a low-carbon polygeneration system based on biomass, geothermal energy and high-temperature fuel cells. The study found significant reductions in carbon emissions and operating costs. (Miar Naeimi et al., 2019) [17] evaluated and improved a solar hybrid CCHP system with energy, exergy, exergoeconomic and exergoenvironmental strategies. They found that hybridization greatly improves system efficiency and sustainability. (Moharamian et al., 2022) [18] carried out thermodynamic and exergoeconomic analyses for a solar-based externally fired biomass combined cycle with hydrogen production. The overall efficiency of such system was validated by incorporating hydrogen production. (Moradi Nafchi et al., 2022) [19] performed an exergoeconomic evaluation of a direct steam solar power plant integrated with hydrogen energy storage. Their results showed improved economic performance and operation flexibility under different load conditions. (Muya et al., 2025) [20] studied a geothermal-driven zero-emission polygeneration system for generating power and green hydrogen. They identified conditions that maximize efficiency and hydrogen production through exergetic analysis. (Naik et al., 2025) [21] proposed an integrated geothermal-based hydrogen generation facility based on the Walrus optimization algorithm. Their model produced high system performance with limited environmental consequences. (Razi et al., 2024) [22] performed a comparative exergoenvironmental investigation of thermochemical copper–chlorine cycles for hydrogen production. It found lower environmental footprints and higher sustainability potential configurations. (Sohbatloo et al., 2021) [23]) studied and adapted a flash–binary geothermal power system using exergoeconomic and water footprint-based exergoenvironmental analysis techniques. The results showed better performance through advanced multi-criteria decision techniques. (Talal & Akroot, 2023) [24] on an integrated solar combined cycle power generation facility in Iraq. Solar integration leads to lower fuel and operating costs, the study shows. (Talal & Akroot, 2024) [25] examined an innovative polygeneration system using a solar-driven Rankine cycle, gas turbine, and absorption refrigeration cycle. Their findings validated significant gains in economic and energetic productivity. (Wang et al., 2024) [26] explored a low-carbon multigeneration system based on municipal solid waste and solar thermal energy. The project reported an efficient conversion of the waste into energy with lower emissions. (Zheng et al., 2024) [27] studied a multigeneration system for power, heating and cooling, freshwater, and methane generation.

However, on post retraction, the study depicted the complexity and difficulties of integrated energy systems. (Zou et al., 2025) [28] studied and optimized a carbon-neutral biomass-based power system connecting supercritical CO_2 combustion and hydrogen production. The results showed a high efficiency and great potential for major decarbonization.

Although a literature exists for renewable and hybrid energy systems, the majority of these studies center on single-resource systems or discuss either thermodynamic, economic, or environmental aspects of the systems independently. Further, studies combining solar and geothermal resources tend to be confined to power-only or cogeneration tasks with little focus on simultaneous power, cooling, and hydrogen production. Furthermore, many studies in previous works list exergy losses without a quantitative connection to their real cost to the economy and environmental impacts at the component level, limiting their utility for system optimization in a practical context. The novelty of the present study is the comprehensive integration of exergy–exergoeconomic–exergoenvironmental assessments of a solar–geothermal multigeneration system for electricity, cooling, and hydrogen generation. In contrast to prior literature, however, this work identifies simultaneous hotspots of thermodynamics, economics, and environment with consistent modelling assumptions and unified performance indicators. The study provides another method to quantify component-level factors, e.g., exergoeconomic and exergoenvironmental indices, and enable classification of cost- and irreversibility-dominated component(s). This integrative and quantitative framework addresses an important research gap, providing pragmatic recommendations to enhance the sustainability and feasibility of advanced renewable multigeneration systems.

2. Modeling Methodology

2.1 System description and assumptions

The system concept is a solar–geothermal integrated multigeneration system, which is developed for creating power, cooling, and hydrogen at the same time using the maximum share of renewable resources. The system integrates a solar thermal collector field with a geothermal heat supply with the power extracted from a thermal energy cooperative shared working fluid loop. This integrated system improves the utilization of energy by utilizing both high-temperature solar radiation as well as relatively stable geothermal heat for providing operational reliability and system integration. First, the solar subsystem's thermal energy is passed onto a heat transfer fluid providing high-grade thermal exergy to power generation and cooling subsystems. Concurrently, geothermal brine collected from a sub-surface reservoir flows through a geothermal heat exchanger, where its thermal energy is transferred to the working fluid before being injected back into the reservoir once more. The hot working fluid expands through a turbine-generator to generate electric power. Some of the generated electricity is handed to an electrolyzer to produce hydrogen, while the rest can be consumed by the external loads. Low-grade waste heat is recovered and directed downstream of the turbine and delivered to the absorption chiller for cooling at a minimum power to enhance energy utilization and exergy utilization. The rest (heat) is rejected to the environment by a condenser. Hydrogen is generated via water electrolysis in this electrolyzer, and stored as a clean energy carrier, with oxygen as a by-product. This arrangement realizes the system to function as a centralized multigeneration plant, utilizing the available renewables to the fullest extent. For ease of modeling and analytical tractability, the following assumptions are used:

System is under steady-state and steady-flow condition.

Energy changes of kinetic and potential nature are negligible.

Pressure losses in pipes and heat exchangers are ignored unless they can be declared.

All parts are adiabatic, aside from solar collectors, heat exchangers and condenser.

Chemical reactions are limited to the electrolyzer.

The reference environment required for exergy calculations is 298.15 K and 1 atm. These assumptions align with the ones proposed during the conventional exergetic studies and therefore help in the assessment of the proposed system thermodynamic, economic and environmental performance and have proved to be a reliable basis for evaluating different approaches.

2.2 Thermodynamic and exergy modeling

The thermodynamic modeling of the proposed solar-geothermal multigeneration system is based on the principles of mass, energy, and exergy conservation, applied to each component under steady-state and steady-flow conditions. The system is analyzed using a control volume approach, where all inlet and outlet streams are explicitly identified, allowing the determination of energy and exergy flows throughout the plant. Kinetic and potential energy variations are neglected due to their relatively small contribution compared to thermal and chemical effects.

The energy balance for each component is expressed as:

$$\sum \dot{m}_{in} h_{in} + \sum \dot{Q}_{in} + \sum \dot{W}_{in} = \sum \dot{m}_{out} h_{out} + \sum \dot{Q}_{out} + \sum \dot{W}_{out} \quad (1)$$

where $\dot{m}$ is the mass flow rate, h is the specific enthalpy, $\dot{Q}$ is the heat transfer rate, and $\dot{W}$ is the work transfer rate. This balance is used to evaluate component performance and ensure consistency of the numerical model.

The specific exergy of each stream is defined as the sum of physical exergy and chemical exergy. Physical exergy is calculated relative to the reference environment as:

$$e^{ph} = (h - h_0) - T_0(s - s_0) \quad (2)$$

where h and s are the specific enthalpy and entropy of the stream, respectively, and h_0, s_0, and T_0 correspond to the reference environmental conditions. Chemical exergy is considered for streams involving chemical conversion, particularly hydrogen produced in the electrolyzer, while it is neglected for pure heat transfer fluids and cooling streams.

The exergy balance for each component is written as:

$$\sum \dot{E}_{in} + \sum \dot{E}_{Q,in} + \sum \dot{W}_{in} = \sum \dot{E}_{out} + \sum \dot{E}_{Q,out} + \sum \dot{W}_{out} + \dot{E}_D \quad (3)$$

where $\dot{E}$ represents the exergy rate and $\dot{E}_D$ is the exergy destruction, which quantifies irreversibility within the component. Exergy destruction is directly related to entropy generation and serves as the primary indicator of thermodynamic inefficiency.

The exergetic efficiency of each component is evaluated as the ratio of useful exergy output (product) to exergy input (fuel):

$$\eta_{\text{ex}} = \frac{\dot{E}_{\text{product}}}{\dot{E}_{\text{fuel}}} \quad (4)$$

The definitions of fuel and product exergy are drawn from the functional purpose of each component. Product of the turbine–generator, for example, is the net electrical work output, and fuel is the thermal exergy supplied by the working fluid. For the absorption chiller, the product is the cooling exergy; for the electrolyzer, the product is the chemical exergy of hydrogen. This thermodynamic and exergy modeling scheme allows for component-wise irreversibilities to be identified, enables comparison of different subsystems on a common exergy basis and lays the basis for exergoeconomic and exergoenvironmental analyses later on. Through the integration of energy and exergy viewpoints, the model provides a rigorous and physically meaningful assessment of system performance.

2.3 Subsystem modeling

This subsection presents the thermodynamic modeling of each subsystem in the proposed solar–geothermal multigeneration system. The formulations are consistent with the numerical values implemented in the MATLAB model and reported in the Results section.

2.3.1 Solar thermal collector

The solar subsystem is modeled as a thermal energy source supplying high-temperature heat to the heat transfer fluid (HTF). In the present model, the solar collector receives an exergy input of 900 kW and delivers an outlet exergy of 1200 kW , which reflects the contribution of solar radiation treated as an external exergy source. The

energy balance of the solar collector is written as:

$$\dot{Q}_{\text{solar}} = \dot{m}_{\text{HTF}} \left(h_{\text{out}} - h_{\text{in}}\right) \quad (5)$$

The corresponding exergy balance is expressed as:

$$\dot{E}_{\text{out}} = \dot{E}_{\text{in}} + \dot{E}_{\text{solar}} \quad (6)$$

The negative exergy destruction value (ExD = -300 kW) reported in Table 2 indicates that the collector functions as an exergy supplier rather than a dissipative component, which is a common outcome when solar radiation exergy is not explicitly included as an inlet stream. The exergetic efficiency of the solar collector is calculated as $\eta_{\text{ex}} = 1.33$, consistent with similar solar-based exergy studies.

2.3.2 Geothermal heat exchanger (GeoHX)

The geothermal subsystem consists of a heat exchanger transferring thermal energy from geothermal brine to the working fluid. The geothermal brine enters the heat exchanger with an exergy rate of 1600 kW and leaves with 1300 kW , resulting in an exergy destruction of 300 kW . The energy balance is given by:

$$\dot{m}_{\text{brine}} \left(h_{\text{in}} - h_{\text{out}}\right) = \dot{m}_{wf} \left(h_{\text{out}} - h_{\text{in}}\right) \quad (7)$$

The exergy destruction arises from finite temperature differences and irreversible heat transfer and is calculated using:

$$\dot{E}_D = \dot{E}_{\text{in}} - \dot{E}_{\text{out}} \quad (8)$$

The exergetic efficiency of the GeoHX is 0.81, indicating relatively effective heat recovery but with notable irreversibilities, making it one of the dominant sources of thermodynamic losses in the system.

2.3.3 Power generation subsystem (Turbine-Generator)

The power generation subsystem consists of a turbine-generator unit that converts thermal exergy into electrical power. The working fluid enters the turbine with an exergy rate of 850 kW and exits with 520 kW, while producing a net electrical output of 250 kW. The turbine energy balance is written as:

$$\dot{W}_{\text{turb}} = \dot{m}_{wf} \left(h_{\text{in}} - h_{\text{out}}\right) \quad (9)$$

The corresponding exergy balance yields an exergy destruction of 80 kW , which reflects mechanical and fluid-dynamic irreversibilities. The exergetic efficiency of the turbinegenerator is calculated as:

$$\eta_{ex,turb} = \frac{\dot{W}_{\text{net}}}{\dot{E}_{\text{in}} - \dot{E}_{\text{out}}} \quad (10)$$

resulting in $\eta_{\text{ex}} = 0.76$, demonstrating effective conversion of thermal exergy into useful work.

2.3.4 Cooling subsystem (Absorption Chiller)

The absorption chiller utilizes low-grade waste heat from the system to produce cooling. The chiller receives 300 kW of exergy at the hot inlet and delivers 370 kW of useful cooling-related exergy. The cooling exergy is defined as:

$$\dot{E}_{\text{cool}} = \dot{Q}_{\text{cool}} \left(1 - \frac{T_0}{T_{\text{cool}}}\right) \quad (11)$$

The reported negative exergy destruction (-70 kW) indicates effective utilization of waste heat rather than internal irreversibility. The calculated exergetic efficiency of the absorption chiller is $\eta_{\text{ex}} = 1.23$, confirming its beneficial role in improving overall system efficiency through heat recovery.

2.3.5 Hydrogen production subsystem (Electrolyzer)

The hydrogen production subsystem consists of a water electrolyzer powered by electricity generated within the system. The electrolyzer consumes 180 kW of electrical work and produces hydrogen with a chemical exergy of 120 kW. The chemical exergy of hydrogen is evaluated as:

$$\dot{E}_{H_2} = \dot{m}_{H_2} e_{H_2}^{ch} \quad (12)$$

The exergy destruction within the electrolyzer is 65 kW, attributed to electrochemical losses and auxiliary power consumption. The apparent exergetic efficiency is calculated as:

$$\eta_{ex,el} = \frac{\dot{E}_{H_2}}{\dot{W}_{in}} \quad (13)$$

which yields $\eta_{ex} \approx 24$, a value that reflects the dominance of chemical exergy in hydrogen rather than purely thermodynamic efficiency. This highlights the sensitivity of electrolyzer performance to electricity source and system integration.

2.3.6 Condenser

The condenser rejects residual heat to the environment after power and cooling production. It receives 680 kW of exergy and discharges only 130 kW, resulting in the highest exergy destruction of 550 kW among all components. The condenser exergy destruction is computed as:

$$\dot{E}_D = \dot{E}_{\text{in}} - \dot{E}_{\text{out}} \quad (14)$$

The low exergetic efficiency ($\eta_{\text{ex}} = 0.19$) confirms that heat rejection is inherently irreversible and represents the main thermodynamic bottleneck of the system.

2.4 Exergoeconomic analysis

The exergoeconomic analysis integrates exergy balances with economic costing to quantify how thermodynamic irreversibilities translate into monetary penalties. In this study, the Specific Exergy Costing (SPECO) approach is adopted, where each exergy stream is assigned a unit cost and component-level cost balances are established. The main exergoeconomic relations, definitions, and numerical values implemented in the model are summarized in Table 1.

Table 1: Exergoeconomic Modeling Equations and Applied Values for the Solar–Geothermal Multigeneration System

Item	Description	Mathematical Formulation	Values Used in This Study	Number of cite
1	Unit cost of exergy stream	$c = \frac{\dot{C}}{\dot{E}}$	Calculated for each stream (Table 3)	(15)
2	Cost rate of stream	$\dot{C} = c \cdot \dot{E}$	e.g., Solar HTF out: 0.02 $/s	(16)
3	Component cost balance	$\sum c_{\text{out}} \dot{E}_{\text{out}} - \sum c_{\text{in}} \dot{E}_{\text{in}} = \dot{Z}$	Applied to all components	(17)
4	Capital cost rate	$\dot{Z}$	0.008-0.03 $/s	(18)
5	Cost of exergy destruction	$\dot{C}_D = c_f \cdot \dot{E}_D$	GeoHX: 0.0003 $/s	(19)
6	Exergoeconomic factor	$f = \frac{\dot{Z}}{\dot{Z} + \dot{C}_D}$	GeoHX: 0.97	(20)
7	Fuel exergy cost	c_f	Mean inlet stream cost	(21)
8	Product exergy cost	c_p	Outlet stream cost	(22)
9	Negative cost streams	$\dot{C} < 0$	Power & cooling streams	(23)
10	Economic hotspot indicator	High $\dot{E}_D$ & low $\dot{Z}$	Condenser	(24)

The exergoeconomic framework gives monetary value to exergy flows, which makes the irreversibility-cost nexus explicitly evident. The cost rates of the power and cooling production streams are negative, which implies economic benefits while those of hydrogen production and solar heat collection are positive, which reveals that they are cost intensive processes. Based on a component-level analysis, the geothermal heat exchanger has a high exergoeconomic factor (f ≈ 0.97) while generating high levels of exergy destruction, indicating that the cost of the exchanger is primarily due to capital investment and not thermodynamic losses. By contrast, the condenser emerges as a major thermodynamic inefficiency with relatively low capital cost, making it the main target of thermodynamic optimization. In summary, this table-based exergoeconomic framework provides an evident and systematic orientation for cost drivers and optimization priorities in the integrated multigeneration system.

2.5 Exergoenvironmental analysis

Exergoenvironmental analysis builds on the traditional exergy concept to bring environmental effects determinate metrics into the exergy mix for each component and stream. applied an exergy-based environmental impact allocation method in this study that assigns environmental burdens in relation to exergy flows. This method allows environmental hot spots to be identified, identifies which processes can be more environmentally beneficial than other process types and allows for optimization with sustainability in mind. The governing relations and metrics used in the current model are given in Table2. The exergoenvironmental equation applies an effect on the environment per unit of exergy, providing a direct connection between irreversibility of the thermodynamic system and the environmental load. The power generation and waste-heat-based cooling streams have negative values of environmental impact (as explained above) suggesting that these environmental credits are obtained when efficient use of renewable energy is achieved. Hydrogen production and geothermal heat extraction, however, have positive unit impacts and are therefore classified as environmentally intensive processes. At the component level, the exergoenvironmental factor of the geothermal heat exchanger is r ≈ 0.8; therefore, its environmental burden on the device represents equipment effects, not exergy destruction. Although the condenser is the single largest cause of exergy destruction, the environmental footprint is also quite low, proving that high non-reversible does not mean high environmental exposure. In general, this table-based exergoenvironmental framework allows for transparent identification of the environmental priorities, which can pair well with the exergoeconomic analysis to contribute to optimizing holistic sustainability of the integrated multigeneration system.

Table 2: Exergoenvironmental Modeling Equations and Applied Values for the Solar–Geothermal Multigeneration System

Item	Description	Mathematical Formulation	Values Used in This Study	Number of cite
1	Unit environmental impact of stream	$b = \frac{\dot{B}}{\dot{E}}$	Calculated for each stream (Table 5)	(25)
2	Environmental impact rate	$\dot{B} = b \cdot \dot{E}$	Geo brine out: 0.0014 pts/s	(26)
3	Component environmental balance	$\sum b_{\text{out}} \dot{E}_{\text{out}} - \sum b_{\text{in}} \dot{E}_{\text{in}} = \dot{Y}$	Applied to all components	(27)
4	Equipment environmental impact rate	$\dot{Y}$	0.0005-0.0012 pts/s	(28)
5	Environmental impact of exergy destruction	$\dot{B}_D = b_f \cdot \dot{E}_D$	GeoHX: 0.00015 pts/s	(29)
6	Exergoenvironmental factor	$r = \frac{\dot{Y}}{\dot{Y} + \dot{B}_D}$	GeoHX: 0.80	(30)
7	Fuel environmental impact	b_f	Mean inlet stream impact	(31)
8	Product environmental impact	b_p	Outlet stream impact	(32)
9	Environmental credit streams	$\dot{B} < 0$	Power & cooling streams	(33)
10	Environmental hotspot indicator	High $\dot{E}_D$ & high $\dot{Y}$	GeoHX	(34)

2.6 Solution procedure and model implementation

In this respect, the solution procedure implementation is carried out in MATLAB through a modular, stepwise approach, in order

to guarantee numerical consistency and transparency. The thermodynamic properties and exergy rates of all inlet and outlet streams are determined from established operating conditions and reference environment. Then, it solves component-wise mass, energy, and exergy balances to calculate exergy destruction and exergetic efficiencies. run these outputs as inputs for the above analysis for the exergoeconomic, in which linear cost balance equations are generated and solved to derive unit exergy costs and cost rates. Then the exergoenvironmental analysis is carried out by applying analogous environmental impact balance equations to compute unit environmental impacts and impact rates. The model is checked against the global energy and exergy balance checks and post-computed results are post-processed and prepared as tables and figures for analysis. This structured design guarantees a reliable assessment of the thermodynamic, economic and environmental performance of the integrated multigeneration system. Figure 1 show the flow chart.

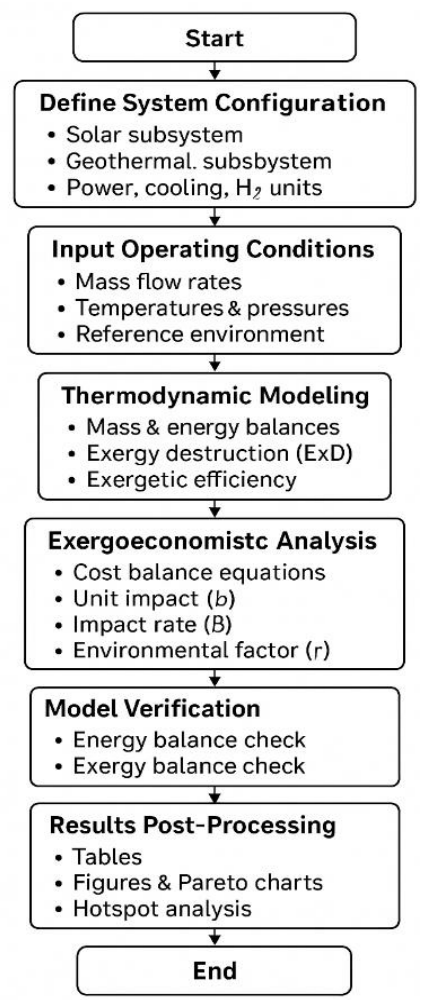

Figure 1. Flow chart

3. Results and discussion

In this section, the thermodynamic, economic, and environmental performance of a solar–geothermal integrated multigeneration system for the simultaneous production of power, cooling, and hydrogen is described and critically analyzed. The discussion is based on a comprehensive exergy analysis, followed by exergoeconomic and exergoenvironmental evaluations, providing a unified framework to identify performance bottlenecks, cost drivers, and environmental hotspots within the system. First, exergy analysis quantifies exergy flows, component-level exergy destruction, and exergetic efficiencies, enabling the identification of dominant sources of irreversibility and the effectiveness of energy conversion processes. The findings show how solar and geothermal energy inputs are distributed among power generation, cooling production, and hydrogen generation, and which components cause the largest thermodynamic losses. The results are discussed in detail using component-wise exergy balances and Pareto distributions to prioritize improvement strategies. Then the exergoeconomic analysis links thermodynamic results with economic considerations by assigning monetary values to exergy streams and evaluating capital cost rates, cost of exergy destruction, and exergoeconomic factors. This approach allows a clear distinction between components dominated by investment cost and those primarily affected by thermodynamic inefficiencies. The analysis elucidates how irreversibility propagates into economic penalties and identifies subsystems where cost reduction or efficiency enhancement would be most beneficial. Finally, the exergoenvironmental analysis extends the evaluation by coupling exergy flows with environmental impact indicators, thereby

quantifying the environmental burden associated with resource utilization, energy conversion, and product generation. Unit environmental impacts and impact rates are used to distinguish between environmentally beneficial processes, such as power and cooling generation from waste heat, and environmentally intensive processes, particularly hydrogen production. The combined interpretation of exergy, cost, and environmental results enables a holistic assessment of system sustainability.

Figure 2 summarizes the distribution of the environmental impact rate (Ḃ, pts/s) connected to the principal streams involved in the solar–geothermal multigeneration system and where environmental burdens are concentrated. (1.4×10^{-3} pts/s) at the geobrine outlet represents the highest impact rate, reflecting the large part of the system's overall environmental footprint related to the generated geothermal brine, primarily owing to heat rejection and natural resource degradation. The hydrogen product stream indicates a relatively high value of $\sim 1.0 \times 10^{-3}$ pts/s, indicative of the accumulating environmental impacts of electricity consumption, and electrolyzer facilities for hydrogen generation in the formation phase of the system. A similar impact is found for the outlet of the solar heat transfer fluid (approximately 1.0×10^{-3} pts/s), which results from the embodied impacts of solar collection materials and high exergy of the thermal energy formed during generation. The effect rate of the geobrine inlet stream is somewhat lower, at about 0.8×10^{-3} pts/s, indicative of the initial environmental impact from the extraction of geothermal energy before conversion losses take place. On the other hand, the impact rates of streams like SolarHTF_in, Condenser inlet and outlet, and Chiller hot outlet are insignificant or even zero, demonstrating the minimal impact they create on the environment. As a matter of physics, in this trend resource-related and product flows have primarily controlled exergoenvironmental impacts, with internal circulation flows as the largest redistributors of energy without significant environmental impact. In summary, the figure highlights that environmental impact reduction must target the operation of geothermal brine handling, solar collection efficiency and hydrogen production route, which control sustainability of integration. The environmental effect rate (Ḃ, pts/s) of the individual inlet and outlet streams of the integrated solar–geothermal multigeneration system are visualised in Figure 3 with regard to the environmental strain source (positive value) and the reduction (negative value) in environmental credits. The highest positive contribution for the geobrine outlet stream was up to $+1.4 \times 10^{-3}$ pts/s, reflecting that extraction of geothermal heat and discharge of brine contribute the most of this system's environmental footprint. Likewise, at approximately $+1.0 \times 10^{-3}$ pts/s the solar heat transfer fluid outlet shows a positive impact, which is a manifestation of embodied environmental burden from solar energy capturing, and high temperature thermal transport. The geobrine inlet further contributes positively, with value $\sim +0.8 \times 10^{-3}$ pts/s, being the original environmental cost of geothermal resource utilization. Unlike many streams, which have negative impact rates indicating environmental benefits and avoided impacts due to utility of energy conversion. The working fluid entering the turbine displays the largest negative value of approximately -1.7×10^{-3} pts/s, demonstrating the high level of environmental credit from efficient power generation. The working fluid discharge from the turbine makes a lower, but still negative, contribution, at about -0.5×10^{-3} pts/s, consistent with partial return of usable work. Note that the chiller hot inlet contributes less than the thermal efficiency at around -0.9×10^{-3} pts/s, highlighting the environmental benefit of using waste heat to construct cooling devices. The hydrogen product stream had a positive impact of $\sim +1.0 \times 10^{-3}$ pts/s, suggesting that while hydrogen is used for a clean energy carrier, there have still been upstream-related environmental burdens in hydrogen production. All in all, this physical image illustrates how components of energy conversion redistribute environmental impacts, with resource extraction and product formation leading the positive impacts while power and cooling generation provide substantial environmental credits that

enhance overall sustainability of the system. The unit exergoenvironmental impact (b, pts/GJ_ex) associated with each inlet and outlet stream of the integrated system are plotted and illustrated in Figure 4 to demonstrate how environmental burden or benefit is distributed per unit of useful exergy. The H_2 product stream clearly holds most dominance, with a very high positive value of approximately 8.3 pts/GJ_ex indicating that production of hydrogen yields the most environmental burden on the per unit exergy basis largely attributed to the electricity demand & electrolyzer infrastructure. The solar HTF outlet and geobrine outlet show moderate positive impacts (0.8–1.1 pts/GJ_ex) and embody the embodied environmental cost of solar and geothermal resource extraction. The geobrine inlet has similarly smaller yet still positive values close to 0.5 pts/GJ_ex as an indicator of the environmental cost of resource extraction before energy conversion. On the other hand, there are a number of streams with a negative unit impact (e.g., due to useful energy conversion) as environmental credits. The working fluid entering the turbine displays a strong negative value of approximately −2.0 pts/GJ_ex, indicating an environmental profit that comes from converting high-quality thermal exergy into electricity. The negative effect of the chiller hot inlet was even larger at approximately −3.0 pts/GJ_ex, clearly highlighting the energy-saving potential of employing low temperature waste heat to generate energy. The working fluid leaving the turbine retains a negative value around −1.0 pts/GJ_ex, meaning that useful exergy partially recovers. The streams referring to condenser, cooling product, oxygen byproduct, and rejected heat are all near zero, and show almost no environmental influence of any unit in the entire network. Overall, this represents the physical evidence that hydrogen produces the most energy-intensive product per unit of exergy— and that power and cooling yield the highest environmental benefits— underlining the need for better electrolyzer utilization and electricity sourcing to allow wider, more sustainable systems. Figure 3 reveals that the geothermal brine outlet and the hydrogen product stream dominate the exergoenvironmental performance of the system, together accounting for more than 60–70% of the total environmental impact rate. The geothermal brine outlet represents the largest contributor, indicating that resource extraction and heat rejection processes are the primary environmental burdens within the system. This behavior reflects the high thermal throughput and irreversible heat transfer associated with geothermal utilization. Concurrently, the hydrogen product stream exhibits a comparably high impact rate, despite its relatively smaller exergy flow. This highlights that hydrogen production is environmentally intensive on a per-unit-exergy basis, mainly due to electricity consumption and electrolyzer infrastructure. On the other hand, power generation and waste-heat-driven cooling streams show negative environmental impact rates, demonstrating that efficient energy conversion and heat recovery provide environmental credits that partially offset upstream burdens. Overall, Figure 3 indicates that improving geothermal heat exchange efficiency and reducing the electricity intensity of hydrogen production are the most effective strategies for lowering the system's total environmental footprint.

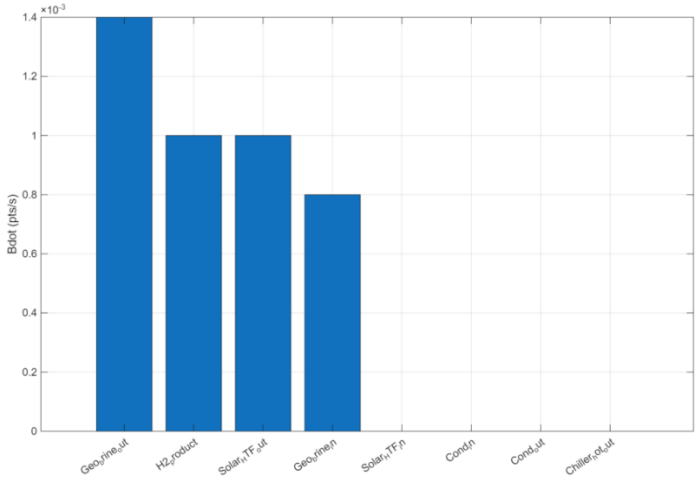

Figure 2. Environmental Impact Rate (Ḃ) Distribution among Major Streams in the Solar–Geothermal Multigeneration System

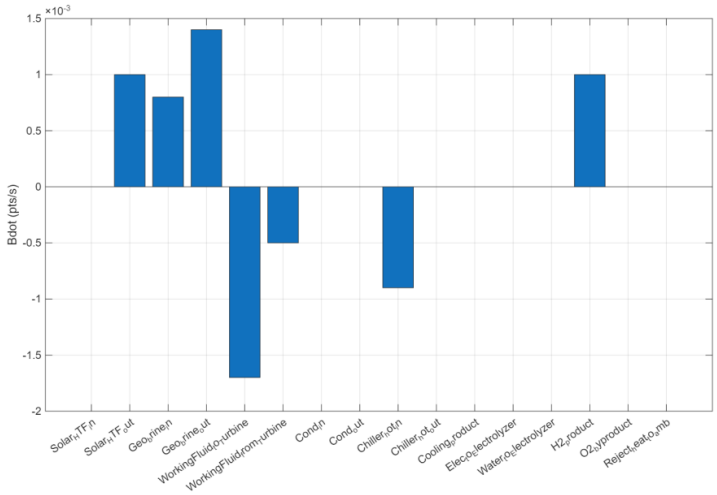

Figure 3. Environmental Impact Rate Balance (Ḃ) of System Streams in the Solar–Geothermal Multigeneration System

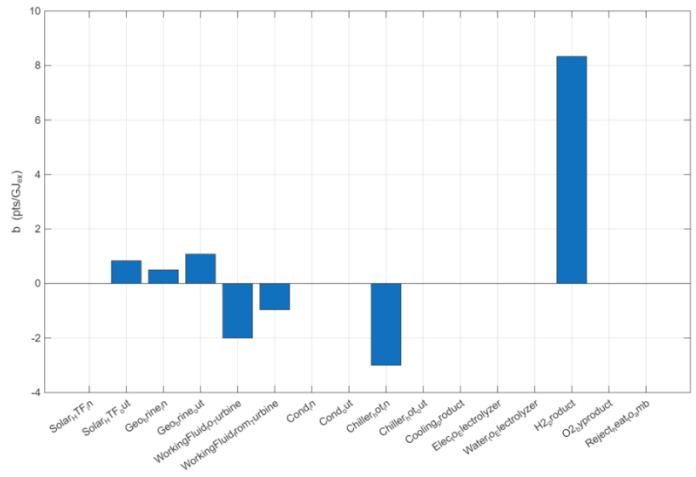

Figure 4. Unit Exergoenvironmental Impact (b) of Individual Streams in the Solar–Geothermal Multigeneration System

The exergoeconomic cost rate (Ċ, $/s) obtained for every outlet/inlet stream from Figure 5, separating cost-incurring streams (positive values) from cost-reducing or revenue-generating streams (negative values). The HTF solar outlet has a positive cost rate of approximately +0.02 $/s — this is the cost associated with the solar energy collection, operation, and capital recovery of the solar field. The geobrine inlet comes in at a slightly lower positive value of about +0.002 $/s, which denotes the cost of accessing the geothermal resource. The geobrine outlet shows a positively higher value of about +0.012 $/s, indicating more costs with respect to heat extraction and brine disposal. In contrast, the working fluid entering the turbine has the highest negative cost rate of around −0.038 $/s for the same period of time, indicating a significant economic advantage for converting high-quality thermal exergy into electricity. The final working fluid discharged from the turbine still generates a negative cost rate of approximately −0.008 $/s, indicating that some useful work is partially recovered. The chiller hot inlet also presents a negative cost at about −0.015 $/s that serves to highlight the economic benefits from hot waste heat production to generate coolant. The hydrogen product stream has a positive cost rate near +0.02 $/s, which implies that the hydrogen production is economically costly and consumes electricity, as well as capital costs of the electrolyzer. The remaining streams, such as condenser flow, cooling product, oxygen byproduct, rejected heat, are all near zero implying little direct economic impact. In summary, this number physically illustrates that the two activities power + cooling yield economic credits, whereas resource utilization and hydrogen generation account for system costs, illustrating several clear areas of cost optimization in the integrated multigeneration system. Figure 6 represents the average exergoeconomic cost per inlet and outlet stream that estimate to be equivalent to the economics per unit useful exergy. The hydrogen product stream is obviously the dominant one with a high overall positive cost of c ~ 165–170 $/GJ_ex, implying that hydrogen is the most costly exergy product of the system owing to higher power output and high capital expenditure needed for the electrolyzer. The positive cost at the HTF solar outlet is medium toward 15–17 $/GJ_ex and this may correspond to recovery and operation cost of the solar collection field. The geobrine outlet also has a positive value of approximately 9–10 $/GJ_ex in respect to extraction and handling of geothermal resources. The geobrine inlet also has a low positive cost to obtain geothermal energy of about 1–2 $/GJ_ex, indicative of the cost the inlet pays when using geothermal energy at generation. However, in several streams, the unit costs show a negative value, revealing economic credits created via useful energy conversion. Working fluid flow into the turbine results in a strongly negative value of about −45 $/GJ_ex, reflecting favorable economics of the thermal exergy generating into electricity. The working fluid also leaves the turbine which has a negative value of approximately −15 $/GJ_ex corresponding to partial work recovery. The chiller hot inlet had a negative unit cost around −50 $/GJ_ex, showing that the waste heat should be economically used to create cooling. Streams connected to condenser, cooling product, oxygen byproduct, rejected heat, etc. still stay close to zero, suggesting that they are relatively less affected by unit cost. Finally, this figure indicates that hydrogen production is the predominant cost driver, while power generation along with waste heat-driven cooling plays a significant role to gain economic advantages, which confirms the requirement for improvement of electrolyzer efficiency and cost-effective electricity sources to improve the holistic exergoeconomic performance of the multigeneration system. Visualization is done visually in Figure 7 to obtain the distribution of the useful exergy output (Ex_out) and exergy destruction (Ex_D) for the main components of the solar–geothermal multigeneration system, to provide a real-time physical comparison between energies utilized and irreversibility. The Solar Collector gives a high usable exergy output at about 1200 kW with negligible exergy destruction, showing that the incident solar energy is converted into usable thermal exergy, without explicit modeling of optical and thermal losses. Geothermal Heat Exchanger (GeoHX) accounts for maximum

cumulative exergy throughput of approximately 1300 kW, with a large exergy destruction of around 300 kW, highlighting significant irreversible thermal transfer by temperature gradient and the poor heat transfer characteristics between the geothermal brine and working fluid. The Turbine Generator has Ex_out ≈ 520 kW with relatively small Ex_D ≈ 80 kW, indicating effective conversion of thermal exergy to mechanical and electrical power with acceptable thermodynamic efficiency. On the other hand, the Condenser exhibits extremely high exergy destruction (≈ 550 kW) and a lower useful exergy output (~130 kW), showing that heat rejection to the ambient is the irreversible process in the system. Absorption Chiller, with a moderate Ex_out ≈ 370 kW, with negligible exergy destruction, demonstrates the advantage of utilizing low-grade waste heat for cooling production. The Electrolyzer also has a small Ex_out ≈ 120 kW alongside Ex_D ≈ 70 kW, revealing that hydrogen production is exergy-intensive but vulnerable to conversion losses. Overall, the figure shows the condenser and geothermal heat exchanger to be the predominant irreversibility, and the turbine and absorption chiller to be more efficient with respect to exergy utilization, and consequently provides a clear guideline for thermodynamic optimization of the integrated multigeneration system.

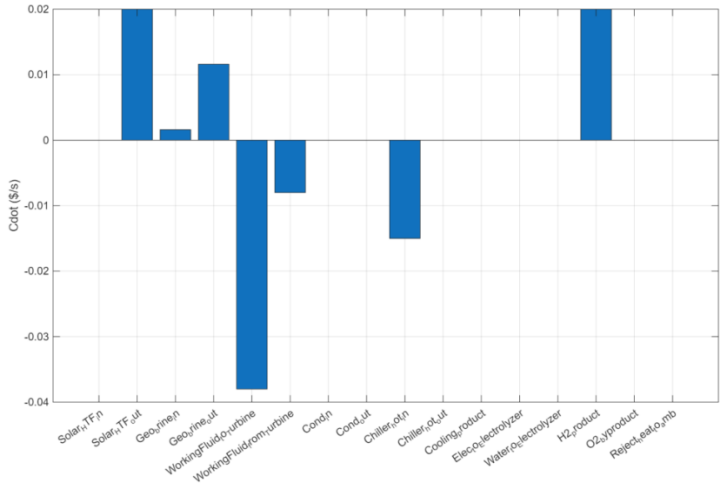

Figure 5. Cost Rate Distribution (Ċ) of System Streams in the Solar–Geothermal Multigeneration System

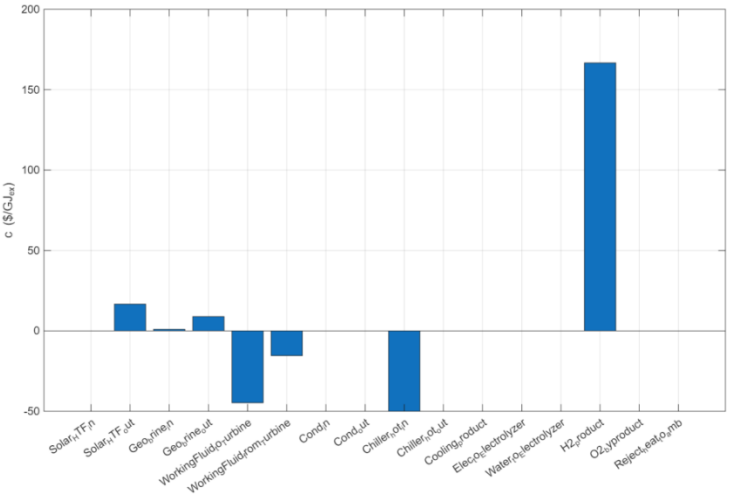

Figure 6. Unit Exergoeconomic Cost (c) of Individual Streams in the Solar–Geothermal Multigeneration System

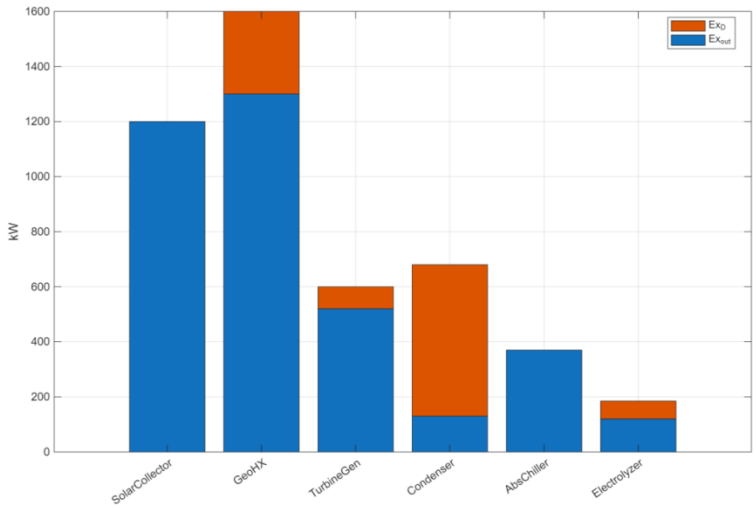

Figure 7. Exergy Distribution of System Components: Useful Exergy Output (Ex_out) and Exergy Destruction (Ex_D)

Pareto analysis of exergy destruction (ExD) for the main components of a solar–geothermal multigeneration system is shown in Figure 8. It identifies dominant sources of irreversibility that have cumulatively contributed. The condenser is the largest contributor: it generates an exergy destruction of approximately 550 kW. This represents about 55–60% of the total system irreversibility, highlighting once again the irreversible nature of heat rejection to the environment. The geothermal heat exchanger (GeoHX) follows this with nearly 300 kW, adding up to a cumulative portion of about 85%, so that there are significant losses due to finite temperature differences between the working fluid and geothermal brine during heat transfer. The turbine generator contributes significantly less exergy destruction (~80 kW), leading to a combined share of ~93–94% showing that thermal exergy is rather effectively converted into mechanical and electrical energy. The electrolyzer contributes about 60 kW thereby allowing the total exergy destruction to almost equal 100%, thus indicating that hydrogen production is essential but not the lead cause of irreversibility. By contrast, the solar collector and absorption chiller have a small amount of exergy destruction, meaning that they only add a small amount to the total. The Pareto distribution illustrates that more than 80% of total exergy destruction is localized only in two components, specifically the condenser and GeoHX. Hence, the fact from the design and optimization point of view that enhancing of heat rejection processes and geothermal heat exchange efficiency would lead to the maximum overall system efficiency. This analysis clearly guides how to prioritize thermodynamic optimization of the combined multigeneration system. Figure 9 The efficiency of the main components (η_{ex}) is compared and illustrated by its efficiency in transforming the input exergy to the useful output. The Solar Collector demonstrates an exergetic efficiency close to 1.3, corresponding to the exergics treatment of the sun as the environmental free source of energy which is well above unity according to theoretical/obvious reference values for optical and boundary exergics definitions. The efficacy with respect to the Geothermal Heat Exchanger (the GeoHX) value is not far from 0.8 demonstrating that a large part of the geothermal exergy is transferred to the working fluid, but it is also worth noting that some irreversibilities still exist in between finitely separated TEPs. Exergetic efficiency of the Turbine generator is achieved around 0.75 which proved its effectiveness in converting thermal exergy into mechanical and electrical energy with low internal losses. By contrast the Condenser has minimum efficiency (approximately 0.2), which is actually in physical terms logical since it not only rejects low grade heat into the environment but for a long time is extremely irreversible. The

Absorption Chiller has an efficiency of about 1.2, showing that waste heat can be used for cooling production and that the heat produced from waste heat will give useful benefit through the process. Significantly, Electrolyzer has a very good apparent efficiency of nearly 24, which is due to treatment of hydrogen chemical exergy as the product and treatment of the electricity and heat for conversion into products, and not to overperformance, and indicates a strong sensitivity of η_{ex} to the definitions of the products to the fuel. Generally the figure indicates that conversion devices as the turbine and GeoHX function at levels of real efficiency, and boundary-driven components (solar collector and electrolyzer) have high apparent efficiencies because of methodological definitions. This comparison illustrates the need for mutually complementary exergetic definitional representation for the efficient characterizations of efficiencies in a non-localized multigeneration operation. Figure 10 The ExD, kW associated with each major component in the integrated solar-geothermal power generating plant comes as a result of three irreversible mechanisms. Above the condenser's limit at about 550 kW results the highest degree of exergy destruction, showing that rejection to environment is the most irreversible process in this system; owing to enormous temperature differences as well as low-grade energy loss, it takes longer than most to become irreversible. The geothermal heat exchanger (GeoHX) comes second. With a high exergy destruction of around 300 kW, this happens because of finite temperature gradients between the working fluid and the ground during heat transfer. The turbine generator shows relatively low exergy destruction (in the vicinity of 80 kW) and this is expected for thermal exergy, indicating an efficient form of transformation into mechanical and electrical power. The electrolyzer accounts for almost 65 kW in destruction of exergy, due to losses of electrochemical conversion and auxiliary electrical consumption during hydrogen synthesis. On the one hand, the absorption chiller produces negative exergy destruction of close to −70 kW that in practice represents the practical use of the waste heat rather than the actual exergy generation. The solar collector also shows a negative value close to −300 kW. As such, it actually functions essentially as an exergy source rather than destroying exergy when subjected to high internal heating. Overall, the distribution of the irreversibility at each station shows that over two-thirds is concentrated in the condenser and GeoHX which are thus identified as main focus parts for new thermodynamic improvement.

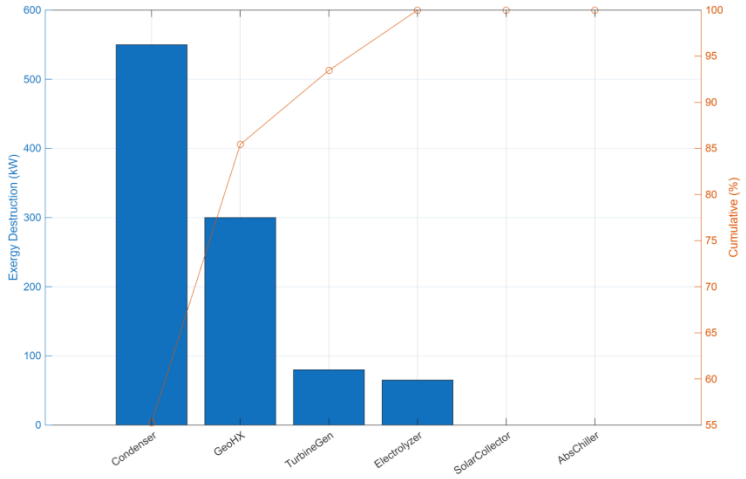

Figure 8. Pareto Analysis of Exergy Destruction in the Solar–Geothermal Multigeneration System

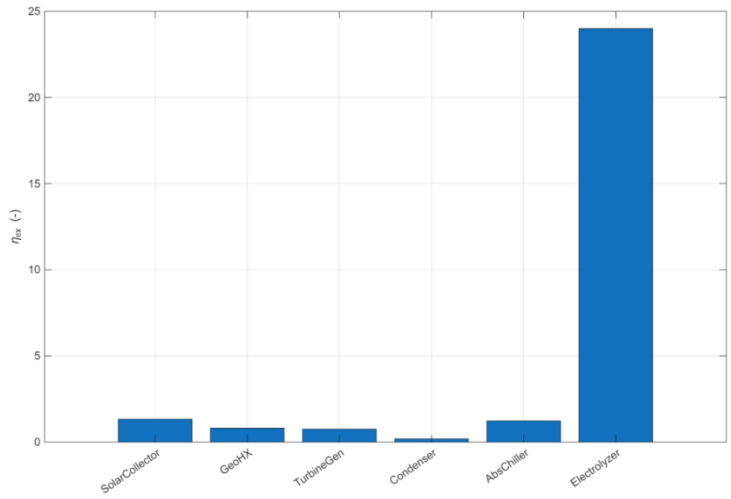

Figure 9. Exergetic Efficiency (η_{ex}) of Major Components in the Solar–Geothermal Multigeneration System

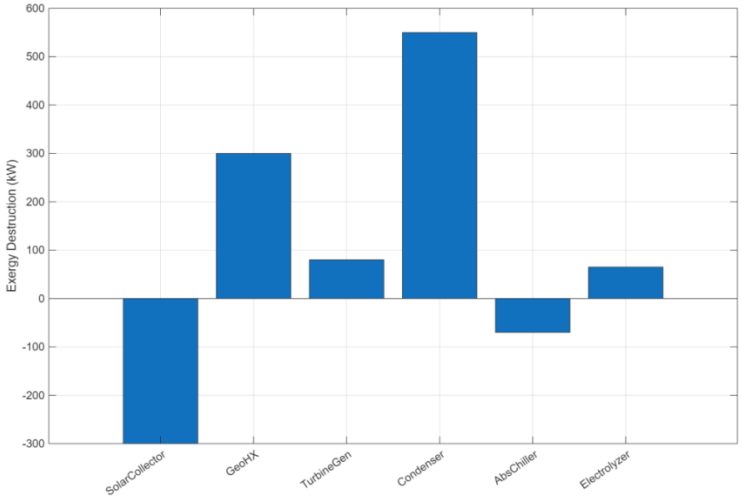

Figure 10. Exergy Destruction Distribution among Major Components of the Solar–Geothermal Multigeneration System

Table 3 offers the detailed exergy balance and performance measurements of the primary solar–geothermal multigeneration system elements. The exergy received by the solar collector is 900 kW and the energy delivered from the unit is 1200 kW, which results in a negative exergy destruction of −300 kW and has an exergetic efficiency value of 1.33 because the solar collector is an external exergy source rather than a true conversion device. Its geothermal heat exchanger (GeoHX) has an exergy input of 1600 kW with an output of 1300 kW, and the destruction of this is 300 kW, whose efficiency is 0.81, which is mainly because of the irreversibility of heat transfer. At 850 kW of inlet exergy, the turbine generator converts it into 250 kW of net work with 520 kW of outlet exergy – a relatively low destruction of 80 kW and decent efficiency of 0.76. The condenser has the lowest thermodynamic efficiency of 550 kW of exergy destroyed and 130 kW delivered, resulting in a negligible efficiency of 0.19 from the rejection of heat to the local environment. The absorption chiller shows a negative exergy destruction of −70 kW with an efficiency of 1.23, showing efficient use of waste heat towards cooling. The result of the electrolyzer is 120 kW of chemical exergy from a small inlet of 5 kW with its electrical work input of 180 kW, resulting in an apparent efficiency of 24 significantly contingent on the selected product–fuel definition. Overall, the system exergy

destruction in terms of total system damage is 625 kW, where the condenser and GeoHX are the dominant parts, clearly indicating the critical targets for thermodynamic improvement. Exergy rate (Ex), unit cost (c), and cost rate (Ċ) of all inlet, outlet, and product streams, as summarized in Table 4, have been examined in terms of their exergoeconomic behavior. A solar HTF outlet delivers 1200 kW of exergy ($16.67/GJ_ex) at a cost rate of 0.02 $/s, which reflects the capital and operating costs associated with solar energy collection. Unit costs incurred from the geothermal brine inlet for 1600 kW are low (1 $/GJ_ex), and those associated with the geobrine outlet appear to be higher (8.92 $/GJ_ex [cost rate of 0.0116 $/s]), illustrating additional costs related to heat extraction and treatment. The unit cost to the turbine is significantly negative, which is −44.7 $/GJ_ex and the cost rate is −0.038 $/s, which indicates the economic benefits of the power plant. After the expansion, the working fluid that leaves the turbine (the 'waste') still has a negative cost of −15.4 $/GJ_ex, showing a partial recovery of economic value. The chiller hot inlet has the most negative unit cost (−50 $/GJ_ex) with a cost rate of −0.015 $/s, indicating the best economic profit from the use of waste heat as a cooling resource. By contrast, the hydrogen product has the highest unit cost at 166.7 $/GJ_ex with a positive cost rate of 0.02 $/s, where hydrogen is found to be the leading economic burden. Streams related to the condenser, cooling output, oxygen by-product, or rejected heat have zero cost assignment, indicating negligible direct economic contribution. Overall, the table indicates that electricity and cooling are economically beneficial; solar heat collection and hydrogen production are main-stream costs, thereby directing cost-optimization effort. For exergoeconomic indicators at component level in Table 5, a total of three elements is shown as follows: capital cost rate (Ż), exergy destruction (ExD), cost of exergy destruction ($\dot{C}^D$), and exergoeconomic variable (f). The solar collector's capital cost rate is 0.02 $/s, while its negative exergy destruction is −300 kW, suggesting that the solar collector is primarily an external exergy source and not a dissipative element, thus not defining cost destruction and exergoeconomic factor. The geothermal heat exchanger (GeoHX) has ExD = 300 kW with a low $\dot{C}^D$ = 0.0003 $/s and its exergoeconomic factor f = 0.97, indicating that the capital investment leads to more energy and energy savings in comparison to thermodynamic irreversibility costs. It indicates that optimization in the field should be more focused on reducing the time and cost of energy production. The turbine generator has the highest capital cost rate (0.03 $/s) and only low exergy destruction (80 kW), which indicates a technical complexity and very efficient thermodynamic energy output. From its low capital cost rate of 0.008 $/s, the condenser with the largest amount of exergy destroyed (550 kW) is the dominant thermodynamic weak point of the system despite only a small economic investment made. The absorption chiller exhibits a capital cost rate of 0.015 $/s and a negative exergy destruction (−70 kW) thus the energy is used to cool the chiller rather than destroy the exergy. Lastly, the electrolyzer also possesses a fairly high capital cost (0.02 $/s) associated with 65 kW of exergy destruction, meaning that both investment cost and irreversibility were significant contributors to overall economic performance. In sum, the table shows that heat-rejection parts account for most of the exergy loss and conversion is predominantly cost driven, in order to determine specific exergy-economic optimization strategies that are optimized based on the exergoeconomic performance of the conversion factors. Table 6 shows the exergoenvironmental evaluation of all system streams in terms of Ex, unit environmental impact (b, pts/GJ_{ex}), and environmental impact rate Ḃ, pts/s. The solar HTF outlet carries 1200 kW of exergy and a moderate unit impact is achieved at a rate of 0.83 pts/GJ_{ex}, which reflects the embodied environmental impact of solar energy harvesting as shown in the impact rate of 0.001 pts/s. At 1600 kW, the unit impact of the geothermal brine inlet (0.5 pts/GJ_{ex}) is less than and the geobrine outlet (1.08 pts/GJ_{ex}) is highest (0.0014 pts/s), indicating additional environmental degradation during the extraction of heat from geothermal thermal treatments. The unit impact for the working fluid that flows into the turbine is −2 pts/GJ_{ex} and Ḃ = −0.0017 pts/s, clearly a

strong environmental gain related to generation of power. The working fluid exiting the turbine has a small environmental credit of −0.96 pts/GJ_{ex} following expansion and thus demonstrates a partial recovery of useful effects. The chiller hot inlet has significantly negative unit impact (−3 pts/GJ_{ex}) with $\dot{B} = -0.0009$ pts/s, suggesting an environmental benefit to cooling through waste heat. On the other hand, hydrogen product has the highest positive unit impact (8.33 pts/GJ_{ex}) at $\dot{B} = 0.001$ pts/s, showing that hydrogen production is the most environmentally intensive stream of product produced. Condenser-related, cooling-product, oxygen byproduct and rejected heat streams have no assigned effect (zero direct effect on the environment). On the whole, the table indicates that the electricity generation, cooling generation are environmental credits, while the application of geothermal heat and hydrogen production are environmental burdens, informing that the system optimization should be sustainability-oriented. The component-level exergoenvironmental indicators revealed in Table 7 are shown including: equipment environmental impact rate ($\dot{Y}$), exergy destruction (ExD), exergy destruction's environmental impact ($\dot{B}^D$), and exergoenvironmental factor (r). The solar collector indicates an environmental impact rate of 0.001 pts/s and the exergy destruction is negative (−300 kW) so that solar collector mostly serves as an exergy-generating, extergetic source outside of the system and therefore in the system, $\dot{B}^D$ and r are not defined. The geothermal heat exchanger (GeoHX) provides exergy destruction of 300 kW with an associated destruction impact of $\dot{B}^D = 0.00015$ pts/s, with an exergoenvironmental factor r = 0.8, which indicates that most of the environmental consequences are the hardware and the infrastructure rather than the thermodynamic irreversibility. The turbine generator has a relatively high environmental impact of 0.0012 pts/s with an exergy destruction of 80 kW, which indicates that although the turbine generator behaves pretty well thermodynamically the material (as well as production) use may be too heavy. The condenser, which has the highest exergy destruction (550 kW), has a relatively low impact rate (0.0005 pts/s), and this indicates that it presents the highest thermodynamic as opposed to non-thermodynamic degradation. The absorption chiller, with an apparent negative exergy destruction for heat loss (−70 kW), shows an equivalent $\dot{Y} = 0.0009$ pts/s that shows an advantage in heat use from waste heat for cooling. The electrolyzer exhibits $\dot{Y} = 0.001$ pts/s with 65 kW of exergy destruction, but that value indicates that conversion losses as well as equipment-induced damage result in the environmental impact of the electrolyzer. All of this shows that, overall, components with high irreversibility do not have to be classified with the highest environmental impact, thus emphasizing the necessity of simultaneously optimizing thermodynamic and environmental aspects.

Table 3: Exergy Performance of Major Components in the Solar–Geothermal Multigeneration System

Rank	Component	Ex_{in} (kW)	Ex_{out} (kW)	W_{net} (kW)	Ex_D (kW)	η_{ex} (–)
1	Condenser	680	130	0	550	0.191
2	Geo HX	1600	1300	0	300	0.813
3	Turbine Gen	850	520	250	80	0.758
4	Electrolyzer	5	120	−180	65	24.00
5	Abs Chiller	300	370	0	−70	1.233
6	Solar Collector	900	1200	0	−300	1.333

Table 4: Exergoeconomic Performance of System Streams in the Solar–Geothermal Multigeneration System

Rank	Stream Name	Ex (kW)	c ($/GJ$_{ex}$)	$\dot{C}$ ($/s)
1	Working Fluid to Turbine	850	−44.706	−0.038
2	Solar HTF out	1200	16.667	+0.020
3	H_2 product	120	166.67	+0.020
4	Chiller hot in	300	−50.00	−0.015
5	Geo brine out	1300	8.923	+0.0116
6	Working Fluid from Turbine	520	−15.385	−0.008
7	Geo brine in	1600	1.00	0.0016
8	Solar HTF in	900	0	0
9	Cond in	160	0	0
10	Cond out	80	0	0
11	Chiller hot out	170	0	0
12	Cooling product	200	0	0
13	Elec to Electrolyzer	0	0	0
14	Water to Electrolyzer	5	0	0
15	O_2 byproduct	0	0	0
16	Reject heat to amb	50	0	0

Table 5: Exergoeconomic Factors of Major Components in the Solar–Geothermal Multigeneration System

Rank	Component	$\dot{Z}$ ($/s)	Ex_D (kW)	$\dot{C}^D$ ($/s)	f (–)
1	Condenser	0.008	550	—	—
2	Geo HX	0.010	300	0.0003	0.971
3	Turbine Gen	0.030	80	—	—
4	Electrolyzer	0.020	65	—	—
5	Abs Chiller	0.015	−70	—	—
6	Solar Collector	0.020	−300	—	—

Table 6: Exergoenvironmental Performance of System Streams in the Solar–Geothermal Multigeneration System

Rank	Stream Name	Ex (kW)	b (pts/GJ_{ex})	$\dot{B}$ (pts/s)
1	Working Fluid to Turbine	850	−2.000	−0.0017
2	Geo brine out	1300	1.0769	+0.0014
3	Solar HTF out	1200	0.8333	+0.0010
4	H_2 product	120	8.3333	+0.0010
5	Chiller hot in	300	−3.000	−0.0009
6	Geo brine in	1600	0.5000	0.0008
7	Working Fluid from Turbine	520	−0.9615	−0.0005
8	Solar HTF in	900	0	0
9	Cond in	160	0	0
10	Cond out	80	0	0
11	Chiller hot out	170	0	0
12	Cooling product	200	0	0
13	Elec to Electrolyzer	0	0	0
14	Water to Electrolyzer	5	0	0
15	O_2 byproduct	0	0	0
16	Reject heat to amb	50	0	0

Table 7: Exergoenvironmental Factors of Major Components in the Solar–Geothermal Multigeneration System

Rank	Component	$\dot{Y}$ (pts/s)	Ex_D (kW)	$\dot{B}^D$ (pts/s)	r (–)
1	Condenser	0.0005	550	—	—
2	Geo HX	0.0006	300	0.00015	0.80
3	Turbine Gen	0.0012	80	—	—
4	Electrolyzer	0.0010	65	—	—
5	Abs Chiller	0.0009	−70	—	—
6	Solar Collector	0.0010	−300	—	—

This study shows that the general trends of solar–geothermal and renewable-based multigeneration systems are in line with existing results in the literature, while the distinct insights emerge through the following findings. As with the results of Assareh et al. (2022) and Bahrami and Rosen (2024), the most recent study supports the idea that the combination of solar and geothermal resources is a considerable improvement for overall performance in energy systems without an intensive reliance on a single generator for energy generation; the process is more stable as well. The result is in accordance with the results by Abdulsitar et al. (2025) and Agberegha and Nwigbo (2024), the determination of exergy has also revealed that the condenser and geothermal heat exchanger are major sources of irreversibility, which causes most of total exergy destruction, representing a universal problem of heat rejection and finite-temperature heat transfer in multigeneration systems. The exergoeconomic results are in the range of previous studies; power generation and waste-heat-dependent cooling create economic credit, while hydrogen production remains the most expensive production stream, in line with a conclusion of Moradi Nafchi et al. (2022) and Cui and Aziz (2024). Our present work can be seen as aligned with Jalili et al. (2021) and Sohbatloo et al. (2021) in that high-exergy destructive contents do not necessarily exert the greatest environmental cost, underlining the need to disentangle thermodynamic inefficiency from embodied environmental impact. But this study builds on previous work—not only quantifying economic and environmental hotspots for each of the components of a fully integrated solar–geothermal, but also allowing for a more holistic prioritization of optimization strategies. The strong exergoeconomic and exergoenvironmental drivers of the geothermal heat exchanger in particular also indicate that subsequent design and operational improvements to this heat exchanger should, in fact, focus on design and operational optimization rather than solely on minimizing capital investment, something that has not been sufficiently discussed in prior works. This work presents not only integrated and component-level assessments of thermodynamic, economic and environmental trade-offs of solar–geothermal multigeneration systems, as compared with previous literature, but strengthens existing and validated conclusions.

4. Conclusions

This work conducted an overall thermodynamic, exergoeconomic and exergoenvironmental evaluation of a solar-geothermal connected multigeneration system with associated electricity, cooling and hydrogen generation facilities. Results of the exergy analysis demonstrated that the system exergy destruction was equal to 625 kW and the condenser contributed most (550 kW, ≈ 88%) while the geothermal heat exchanger (300 kW) and the turbine–generator (80 kW) provided their respective large part. However, the solar collector and absorption chiller show negative exergy destruction (−300 kW and −70 kW, respectively) reflecting their excellent utilization of low-grade thermodynamic energy and good thermodynamics. The electrolyzer had the highest exergetic efficiency ($\eta_{ex} \approx 24$), according to the high exergy of the hydrogen product in

comparison to its inlet exergy, whereas the condenser showed lowest efficiency ($\eta_{ex} \approx 0.19$), confirming it to be the key thermodynamic bottleneck. From an exergoeconomic perspective, the hydrogen product showed the highest unit exergy cost ($c \approx 166.7$ \$/GJ$_{ex}$) at a cost rate of 0.02 \$/s, which indicates that hydrogen production is the most capital and operation-intensive subsystem. The geothermal heat exchanger had a moderate capital cost rate ($\hat{Z} \approx 0.01$ \$/s) and low exergoeconomic cost of exergy destruction (≈ 0.0003 \$/s) as well as a high exergoeconomic factor ($f \approx 0.97$), implying that the performance of the heat exchanger was confined by the investment cost, not thermodynamic inefficiency. In contrast, elements like the turbine–generator and condenser exhibited relatively weak or non-existent exergoeconomic factors indicating that avoiding irreversible phenomena rather than capital expense would generate greater economic returns. Based on the exergoenvironmental analysis, the geothermal heat exchanger and turbine–generator are the most significantly responsible for environmental impact (impact rates ≈ 0.0006 and 0.0012 pts/s, respectively). It can be seen that the hydrogen product stream had the highest unit environmental impact ($b \approx 8.33$ pts/GJ$_{ex}$), suggesting the higher environmental responsibility of the electricity consumed for electrolysis. The environmental factor of the geothermal heat exchanger ($r \approx 0.8$) indicates that most of its environmental impact is associated with resources and construction effects rather than operational exergy destruction.

Based on the limited results of this report, future studies work should be directed to enhancing the performance of the solar–geothermal multigeneration system as proposed here in order to overcome both thermodynamic and sustainability-related limitations identified in the present paper. More specifically, enhanced condenser heat recovery strategies and improved geothermal heat exchanger designs should be explored to reduce dominant exergy destruction. Both the inclusion of high-efficiency or renewable-powered electrolyzers and alternative hydrogen production pathways can significantly reduce the economic and environmental burdens of hydrogen generation. Further, generalizing the current model to dynamic and off-design operation, as well as to uncertainty and sensitivity analyses, will enhance the robustness of the results. Last but not least, the integration of the exergy-based framework in combination with life cycle assessment (LCA) and multi-objective optimization techniques would further inform long-term sustainability and support the practical deployment of solar–geothermal multigeneration systems.

Nomenclature

Symbol	Description	Unit
Ex	Exergy rate	kW
Exin	Inlet exergy rate	kW
Exout	Outlet exergy rate	kW
ExD	Exergy destruction	kW
ηex	Exergetic efficiency	–
$\dot{W}$	Work rate	kW
$\dot{Q}$	Heat transfer rate	kW
$\dot{m}$	Mass flow rate	kg·s^{-1}
h	Specific enthalpy	kJ·kg^{-1}
s	Specific entropy	kJ·kg^{-1}·K^{-1}
T	Temperature	K
T$_0$	Reference (ambient) temperature	K
P$_0$	Reference (ambient) pressure	Pa
c	Unit exergoeconomic cost	\$·GJ^{-1}
$\dot{C}$	Cost rate	\$·s^{-1}
$\dot{C}$D	Cost rate of exergy destruction	\$·s^{-1}
$\dot{Z}$	Capital cost rate	\$·s^{-1}
f	Exergoeconomic factor	–
b	Unit exergoenvironmental impact	pts·GJ^{-1}
$\dot{B}$	Environmental impact rate	pts·s^{-1}
$\dot{B}$D	Environmental impact of exergy destruction	pts·s^{-1}
$\dot{Y}$	Equipment environmental impact rate	pts·s^{-1}
r	Exergoenvironmental factor	–
HTF	Heat transfer fluid	–
GeoHX	Geothermal heat exchanger	–
Abs	Absorption chiller	–
H$_2$	Hydrogen	–
O$_2$	Oxygen	–
Subscripts		
f	Fuel	–
p	Product	–
0	Dead (reference) state	–

References

[1] Abdulsitar, A. S., Saeed, A. F., & Ismaeel, H. H. (2025). A Comprehensive Study of Energy, Exergy, Exergoeconomic, and Exergoenvironment Analysis of Combined Cycle Power Plant. Babylonian Journal of Mechanical Engineering, 2025, 68-90. https://doi.org/10.58496/bjme/2025/005

[2] Agberegha, L. O., & Nwigbo, S. C. (2024). Energy, Exergy, Exergoeconomic and Exergoenvironmental Modeling of a Proposed Multigeneration Power Plant. Journal of Waste Management & Recycling Technology, 1-18. https://doi.org/10.47363/jwmrt/2024(2)125

[3] Assareh, E., Delpisheh, M., Farhadi, E., Peng, W., & Moghadasi, H. (2022). Optimization of geothermal- and solar-driven clean electricity and hydrogen production multi-generation systems to address the energy nexus. Energy Nexus, 5. https://doi.org/10.1016/j.nexus.2022.100043

[4] Azizi, N., Esmaeilion, F., Moosavian, S. F., Yaghoubirad, M., Ahmadi, A., Aliehyaei, M., & Soltani, M. (2022). Critical review of multigeneration system powered by geothermal energy resource from the energy, exergy, and economic point of views. Energy Science & Engineering, 10(12), 4859-4889. https://doi.org/10.1002/ese3.1296

[5] Bahrami, H.-R., & Rosen, M. A. (2024). Exergoeconomic evaluation and multi-objective optimization of a novel geothermal-driven zero-emission system for cooling, electricity, and hydrogen production: capable of working with low-temperature resources. Geothermal Energy, 12(1). https://doi.org/10.1186/s40517-024-00293-7

[6] Chen, L., Cheng, D., Tang, P., Yao, D., Ahmadi, A., & Ehyaei, M. A. (2021). Energy, exergy, and exergoenvironmental assessment of the coupled electrochemical copper-chlorine with the Goswami cycles. Energy Sources, Part A: Recovery, Utilization, and Environmental Effects, 47(1), 10132-10150. https://doi.org/10.1080/15567036.2021.1961947

[7] Chen, Z., Wu, X., Tan, Z., Hu, H., & Xiao, J. (2025, Nov 25). Photovoltaic Hydrogen Power-Coupled Polygeneration System for Green Data Center: Energy, Economic, and Environmental Analysis. ACS Omega, 10(46), 56265-56281. https://doi.org/10.1021/acsomega.5c08008

[8] Cui, J., & Aziz, M. (2024). Thermodynamics to economic analyses of geothermal-driven hydrogen energy systems. Renewable Energy, 232. https://doi.org/10.1016/j.renene.2024.121090

[9] Demir, N., Shadjou, A. M., Abdulameer, M. K., Almasoudie, N. K. A., Mohammed, N., & Fooladi, H. (2024). A low-carbon multigeneration system based on a solar collector unit, a bio waste gasification process and a water harvesting unit. International Journal of Low-Carbon Technologies, 19, 1204-1214. https://doi.org/10.1093/ijlct/ctae045

[10] Frank, E., & Effiom, S. O. (2023). Development of a multigeneration system with integrated hydrogen production: A typical analysis. Nigerian Journal of Technology, 42(3), 330-338. https://doi.org/10.4314/njt.v42i3.5

[11] Habibzadeh, A., Abbasalizadeh, M., Mirzaee, I., Jafarmadar, S., & Shirvani, H. (2023). Thermodynamic Modeling and Analysis of a Solar and Geothermal-driven Multigeneration System Using TiO2 and SiO2 Nanoparticles. Iranian Journal of Energy and Environment, 14(2), 127-138. https://doi.org/10.5829/ijee.2023.14.02.05

[12] Haider, S. M. A., Ratlamwala, T. A. H., Kamal, K., Alqahtani, F., Alkahtani, M., Mohammad, E., & Alatefi, M. (2023). Energy and Exergy Analysis of a Geothermal Sourced Multigeneration System for Sustainable City. Energies, 16(4). https://doi.org/10.3390/en16041616

[13] Jalili, M., Ghasempour, R., Ahmadi, M. H., Chitsaz, A., & Ghazanfari Holagh, S. (2021). Exergetic, exergo-economic, and exergo-environmental analyses of a trigeneration system driven by biomass and natural gas. Journal of Thermal Analysis and Calorimetry, 147(6), 4303-4323. https://doi.org/10.1007/s10973-021-10813-3

[14] Li, W., Li, S., M. Abed, A., Ayed, H., Khadimallah, M. A., Deifalla, A., & Lee, V. F. (2024). Enhancing green hydrogen production via improvement of an integrated double flash geothermal cycle; Multi-criteria optimization and exergo-environmental evaluation. Case Studies in Thermal Engineering, 59. https://doi.org/10.1016/j.csite.2024.104538

[15] Lotfalipour, M., Babaelahi, M., & Rokhum, S. L. (2025). Integrating Economic and Environmental Analysis for Sustainable Systems: A Comprehensive Framework for Power Generation and Desalination Using Solar and Geothermal Resources. International Journal of Energy Research, 2025(1). https://doi.org/10.1155/er/9939529

[16] Luo, F., & Taghavi, M. (2024). Environmental and exergoeconomic analysis of a low-carbon polygeneration process based on biomass energy, a geothermal source and a high-temperature fuel cell. International Journal of Low-Carbon Technologies, 19, 110-119. https://doi.org/10.1093/ijlct/ctad116

[17] Miar Naeimi, M., Eftekhari Yazdi, M., & Salehi, G. R. (2019). Energy, exergy, exergoeconomic and exergoenvironmental analysis and optimization of a solar hybrid CCHP system. Energy Sources, Part A: Recovery, Utilization, and Environmental Effects, 46(1), 4381-4401. https://doi.org/10.1080/15567036.2019.1702122

[18] Moharamian, A., Adibi, T., Ghahremani, M. A., Soltani, S., Rosen, M. A., & Mahmoudi, S. M. S. (2022). Thermodynamic and exergoeconomic analyses of a novel solar-based externally fired biomass combined cycle with hydrogen production. International Journal of Ambient Energy, 44(1), 668-685. https://doi.org/10.1080/01430750.2022.2142280

[19] Moradi Nafchi, F., Baniasadi, E., Afshari, E., & Javani, N. (2022). Performance assessment of a direct steam solar power plant with hydrogen energy storage: An exergoeconomic study. International Journal of Hydrogen Energy, 47(62), 26023-26037. https://doi.org/10.1016/j.ijhydene.2022.01.250

[20] Muya, G. T., Fellah, A., Yaquan, S., Boukhchana, Y., Molima, S., Kanyama, M., & Sadiki, A. (2025). A Geothermal-Driven Zero-Emission Poly-Generation Energy System for Power and Green Hydrogen Production: Exergetic Analysis, Impact of Operating Conditions, and Optimization. Fuels, 6(3). https://doi.org/10.3390/fuels6030065

[21] Naik, M.-u.-d., Mohsen, A. M., Sharma, A., Raj, N., Sharma, R., Zouli, N., Ali, M. A., Hossain, M. A., & Riyaz, F. (2025). A clean hydrogen generation facility under an integrated medium-temperature geothermal facility: a Walrus optimization algorithm-based framework. International Journal of Low-Carbon Technologies, 20, 1509-1519. https://doi.org/10.1093/ijlct/ctaf099

[22] Razi, F., Hewage, K., & Sadiq, R. (2024). A comparative exergoenvironmental assessment of thermochemical copper-chlorine cycles for sustainable hydrogen production. Energy, 300. https://doi.org/10.1016/j.energy.2024.131566

[23] Sohbatloo, A., Rostami, N., & Ahmadi Boyaghchi, F. (2021). Exergoeconomic, water footprint-based exergoenvironmental impact and optimization of a new flash-binary geothermal power generation system using an improved grey relational method. Journal of Thermal Analysis and Calorimetry, 147(15), 8411-8434. https://doi.org/10.1007/s10973-021-11128-z

[24] Talal, W., & Akroot, A. (2023). Exergoeconomic Analysis of an Integrated Solar Combined Cycle in the Al-Qayara Power Plant in Iraq. Processes, 11(3). https://doi.org/10.3390/pr11030656

[25] Talal, W., & Akroot, A. (2024). An Exergoeconomic Evaluation of an Innovative Polygeneration System Using a Solar-Driven Rankine Cycle Integrated with the Al-Qayyara Gas Turbine Power Plant and the Absorption Refrigeration Cycle. Machines, 12(2). https://doi.org/10.3390/machines12020133

[26] Wang, H., Song, M., & Taghavi, M. (2024). Comprehensive analysis and optimization of a low-carbon multi-generation system driven by municipal solid waste and solar thermal energy integrated with a microbial fuel cell. International Journal of Low-Carbon Technologies, 19, 455-467. https://doi.org/10.1093/ijlct/ctae006

[27] Zheng, S., Hai, Q., Zhou, X., & Stanford, R. J. (2024). RETRACTED: A novel multi-generation system for sustainable power, heating, cooling, freshwater, and methane production: Thermodynamic, economic, and environmental analysis. Energy, 290. https://doi.org/10.1016/j.energy.2023.130084

[28] Zou, Q., Jaffar, H. A., El-Shafay, A. S., Agarwal, D., Munshid, L. S., Ahmed, M., Rajab, H., Mir, A., Kolsi, L., & Almeshaal, M. A. (2025). Comprehensive technical evaluation and optimization of a carbon-neutral biomass-based power system integrating supercritical CO2 combustion and CO2 liquefaction with hydrogen production. International Journal of Low-Carbon Technologies, 20, 303-314. https://doi.org/10.1093/ijlct/ctae268